



1 **A new methodology for measuring traveling quasi-5-day**
2 **oscillations during SSWs based on satellite observations**

3
4
5
6
7
8

Zheng Ma^{1,2}, Yun Gong^{1,2}, Shaodong Zhang^{1,2,3,4}, Qiao Xiao^{1,2}, Chunming
Huang^{1,2}, and Kaiming Huang^{1,2}

- 9 1. School of Electronic Information, Wuhan University, Wuhan, China.
10 2. Key Laboratory of Geospace Environment and Geodesy, Ministry of Education,
11 Wuhan, China.
12 3. State Key Laboratory of Information Engineering in Surveying, Mapping and
13 Remote Sensing, Wuhan University, Wuhan, China.
14 4. Guizhou Normal University, Guiyang, China.

15
16
17
18
19

Correspondence to Yun Gong (yun.gong@whu.edu.cn)



20 **Abstract**

21 Enhancements of stationary planetary waves (SPWs) and traveling planetary
22 waves (TPWs) are commonly observed in the middle atmosphere during sudden
23 stratospheric warming (SSW) events. Based on the least square fitting method (Wu et
24 al., 1995), numerous studies have used satellite measurements to investigate the
25 characteristics of TPWs during SSWs but ignored the effect of the SPWs. However, a
26 rapid and large change in the SPWs during SSWs may lead to significant disturbances
27 in the amplitude of derived TPWs. In this study, we present a new methodology for
28 obtaining the amplitudes and wavenumbers of traveling quasi-5-day oscillations
29 (Q5DOs) in the middle atmosphere during major SSWs. Our new fitting method is
30 developed by inhibiting the effect of a rapid and large change in SPWs during SSWs.
31 We demonstrate the effectiveness of the new method using both synthetic data and
32 satellite observations. The results of the simulations indicate that the new method can
33 suppress the aliasing from SPWs and capture the real variations of TPWs during SSWs.
34 Based on the geopotential height data measured by the Aura satellite from 2004 to 2021,
35 the variations of traveling Q5DOs during eight mid-winter major SSWs are reevaluated
36 using the new method. The differences in the fitted amplitudes between the least square
37 fitting method and the new method are usually over 100 m during the SSW onsets. Our
38 analysis indicates that previously-reported Q5DOs during SSWs might be
39 contaminated by SPWs, which leads to both overestimation and underestimation in the
40 amplitudes of the traveling Q5DOs.

41



42 **1. Introduction**

43 Sudden stratospheric warming (SSW) is one of the most representative phenomena
44 in the atmospheric dynamics in the polar region, which is excited by the interaction
45 between stationary planetary waves (SPWs) and background mean flow (Matsuno,
46 1971; Baldwin et al., 2020). The onset of SSW is characterized by a positive
47 temperature gradient of zonal mean temperature between 90°N and 60°N at 10 hPa
48 (Andrews et al., 1987). Generally, a major SSW event is additionally associated with
49 the phenomenon of wind reversals in the zonal mean eastward winds at 60°N and 10
50 hPa; otherwise, SSWs are regarded as minor events (Charlton and Polvani, 2007; Butler
51 et al., 2017; Choi et al., 2019). During the occurrence of SSWs, the enhancements of
52 SPWs largely affect the energy transportation in the stratosphere and the occurrence of
53 extreme weather in the troposphere at middle latitudes (e.g., Manney et al., 2009;
54 Kozubek et al., 2015; King et al., 2019; Domeisen et al., 2020). The zonal wavenumber
55 of the enhanced SPWs usually corresponds to the geometry of the polar vortex during
56 SSWs. A displacement vortex is mainly due to a strong SPW with a zonal wavenumber
57 of 1 (SPW1) and split vortices are always associated with large SPWs with a zonal
58 wavenumber of 2 (SPW2) (e.g., Seviour et al., 2013; Lawrence and Manney, 2018;
59 Choi et al., 2019).

60 Traveling planetary waves (TPWs), widely observed with strong amplitudes
61 during SSWs in recent decades, also play a significant role in controlling the global
62 atmospheric and ionospheric couplings during SSWs (e.g., Gong et al., 2019; Koushik
63 et al., 2020; Lin et al., 2020; Ma et al., 2022). One of the prominent TPWs, the westward



64 propagating quasi-5-day oscillation (Q5DO) with periods of 4-7 days, is usually
65 observed from the mesosphere to the ionosphere at mid-latitudes during SSWs with the
66 zonal wavenumbers both 1 and 2 (W1 and W2) (Gong et al., 2018; Pancheva et al.,
67 2018; Yamazaki et al., 2020, 2021). These Q5DOs are believed to be generated by
68 atmospheric barotropic/baroclinic instability due to large changes in zonal winds and
69 temperatures during SSWs (e.g., Liu et al., 2004; Ma et al., 2020; Yamazaki et al., 2021).
70 Based on the least square fitting method introduced by Wu et al. (1995), the amplitude,
71 phase, and zonal wavenumber of the Q5DOs can be obtained from satellite observations
72 and reanalysis data sets (e.g., Huang et al., 2017; Qin et al., 2021). However, based on
73 the least square fitting method, a rapid and large change in the amplitudes of SPWs
74 would lead to an apparent fluctuation in the amplitude of TPWs over a broad range of
75 frequencies, including those corresponding to Q5DOs. Yamazaki and Matthias (2019)
76 proposed that based on the least square fitting method, the effect of an SPW on a quasi-
77 10-day wave (Q10DW) is equivalent to two oppositely propagating waves with equal
78 amplitudes, periods, and wavenumbers. They suggested that the effect of SPWs can be
79 ignored when the activities of Q10DWs in the oppositely propagating direction were
80 not simultaneously enhanced.

81 However, the rapid change in the amplitudes of SPWs is a typical characteristic
82 during the occurrence of SSWs. Previous studies usually ignored the effect of SPWs
83 when obtaining the amplitudes of Q5DOs from satellite observations (e.g., Gong et al.,
84 2018; Qin et al., 2021). Nevertheless, both westward and eastward Q5DOs have been
85 frequently reported during SSWs in recent years (e.g., Pancheva et al., 2018; Rhodes et



86 al., 2021; Wang et al., 2021; Yu et al., 2022). Thus, it is necessary to understand the real
87 physics of the enhanced Q5DOs during SSWs and their relationships with SPWs. It is
88 also necessary to inhibit the effect of SPWs when studying the variations of Q5DOs
89 during SSWs. In the present study, we develop a new method for measuring the
90 variation of westward and eastward propagating Q5DOs by inhibiting the effect of a
91 rapid and large change in SPWs. The effectiveness of the new method is demonstrated
92 by using both simulations and satellite observations. The paper is organized as follows.
93 In Section 2, the synthetic data and the satellite data used in this study are introduced.
94 Section 3 presents the new methodology for measuring the amplitudes of Q5DOs.
95 Discussions are given in Section 4, mainly focusing on the comparisons of traveling
96 Q5DOs during SSWs between the least square fitting method and the new fitting
97 method. Conclusions are summarized in section 5.

98 **2. Data**

99 In the present study, a simulation is performed based on synthetic data to further
100 understand the issue of SPWs and Q5DOs during SSWs. The synthetic data $Y(x, t)$
101 are built based on equation (1), including three components: an SPW, a westward
102 propagating Q5DO, and an eastward propagating Q5DO, respectively, which is
103 expressed as:

$$104 Y(x, t) = A_k(t) \cos(kx - \varphi_k) + B_w \cos(\omega t + kx - \varphi_w) + B_e \cos(\omega t - kx - \varphi_e) \quad (1)$$

105 where x is the longitudes, t is the time, k is the wavenumber, ω is the frequency of
106 Q5DOs, A_k and φ_k are the amplitude and phase of SPWs, B_w and B_e denote the



107 amplitudes of westward and eastward Q5DOs with the phase of φ_w and φ_e ,
108 respectively. Based on the least square fitting method introduced by Wu et al. (1995),
109 TPWs with the same zonal wavenumber but in other periods only cause periodic
110 modulation in the fitted amplitudes of Q5DOs. The aliasing caused by TPWs with
111 different wavenumbers is mainly captured in the studies of quasi-2-day waves based on
112 satellite measurements (Tunbridge et al., 2011). For the analysis of Q5DOs, the aliasing
113 caused by TPWs with different wavenumbers is usually ignored, because Q5DOs with
114 wavenumbers of 3 or 4 are rarely reported. Nevertheless, the most important issue of
115 the least square fitting method may be the aliasing due to the rapid and large changes
116 in the SPWs. Therefore, to better understand the issue, the synthetic data for the
117 simulations in the present study only includes three components of waves with the same
118 zonal wavenumbers.

119 To verify the effectiveness of different fitting methods, the geopotential height data
120 measured by the Aura/Microwave Limb Sounder (MLS) from 2005 to 2021 are used to
121 derive the Q5DOs in the present study. The available Aura/MLS geopotential height
122 data in the version 4.2x Level 2 product is from 261 hPa to 0.001 hPa (Livesey et al.,
123 2017), with the measurement errors of ± 25 m, ± 45 m, ± 110 m, and ± 160 m at 1 hPa,
124 0.1 hPa, 0.01 hPa, and 0.001 hPa. A comprehensive study of the measurement errors
125 and fitting errors has been reported by Yamazaki and Matthias (2019) when using the
126 Aura/MLS geopotential height data to obtain the amplitudes of Q5DOs. They have
127 suggested that the mean values of the estimated $1-\sigma$ uncertainties in TPWs are about 50
128 m at high latitudes in the Northern Hemisphere. Following their technique, mean values



129 of the estimated $1\text{-}\sigma$ uncertainties in the fitted amplitudes obtained by the new method
130 are also about 50 m. The vertical structure of the estimated $1\text{-}\sigma$ uncertainty of the new
131 method is the same as the distributions shown in Yamazaki and Matthias (Figure 1,
132 2019). In the present study, we focus on the difference between the original and new
133 fitting methods. The fitted amplitudes are presented in the following analyses without
134 dropping the values that are lower than the uncertainties. The analysis of this study
135 focuses on the traveling Q5DOs with zonal wavenumbers of 1 and 2 based on the data
136 at 60°N (averaged from $55\text{-}65^\circ\text{N}$).

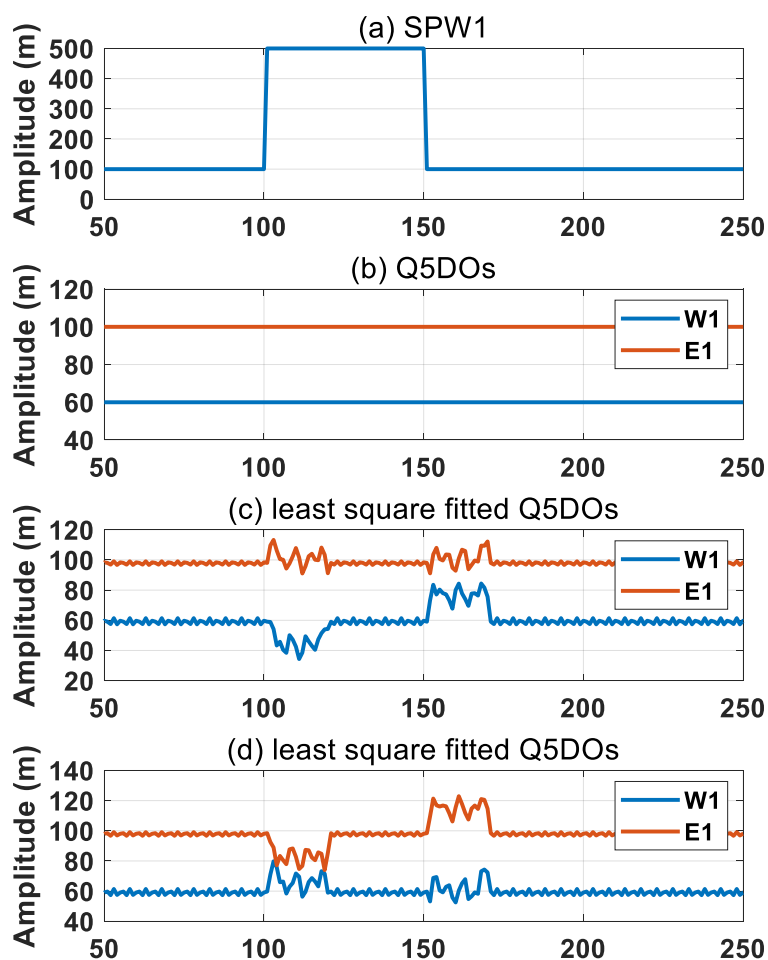
137 **3. Methodology**

138 **3.1 Simulations of the least square fitting method**

139 The least square fitting method used in previous studies to derive the amplitude
140 and phase of Q5DOs from satellite observations is based on equation (1) but without
141 fitting the first term on the right-hand side (e.g., Huang et al., 2017; Qin et al., 2021).
142 Generally, a 20-day sliding window with a step of one day is used to simultaneously
143 extract the amplitudes of TPWs with zonal wavenumbers from 3 to -3 (westward to
144 eastward). The daily amplitudes of the Q5DOs are obtained with the largest value in
145 the wave periods between 4 and 7 days. To better understand the original least square
146 fitting method, the synthetic data are used to firstly simulate the effect of a rapid and
147 large change in SPWs when calculating the amplitudes of Q5DOs. As shown in Figures
148 1a and 1b, three components of waves with the zonal wavenumber of 1 are given in the
149 synthetic data, which are an SPW with the amplitude of 100 m, eastward and westward



150 propagating Q5DOs with amplitudes of 100 m and 60 m, respectively. The phases are
151 respectively set as 0, $-\pi/4$, and $\pi/5$ for the SPW and the westward and eastward
152 propagating Q5DOs. To simulate the effect of SPWs on TPWs, rapid large changes are
153 given in the amplitudes of SPW on day 100 with magnitudes from 100 m to 500 m and
154 on day 150 with magnitudes from 500 m to 100 m (see Figure 1a).



155

156 Figure 1. Simulations of the least square fitting method based on synthetic data, which



157 includes an SPW and westward and eastward Q5DOs with zonal wavenumber of 1. (a)
158 Daily variations of the SPW amplitudes. The phase of the SPW is 0. (b) The real
159 amplitudes of Q5DOs. Amplitudes are separately set as 100 m and 60 m for the
160 eastward and westward Q5DOs. (c) Q5DOs obtained from the least square fitting
161 method. The phases are $-\pi/4$ and $\pi/5$ for the westward and eastward Q5DOs,
162 respectively. (d) Same as (c) but with phases of $\pi/4$ and $-\pi/5$ for the westward and
163 eastward Q5DOs.

164 Figure 1c presents the amplitudes of the westward and eastward propagating
165 Q5DOs fitted by the least square fitting method. As shown in Figure 1c, abnormal
166 fluctuations after day 100 and day 150 are captured, which correspond to the occurrence
167 of rapid large changes in the amplitudes of SPW. However, Figure 1c suggests that the
168 fitted Q5DOs are not largely influenced by the SPWs when rapid large changes are not
169 given in the amplitudes of SPWs (before day 100 or from day 120 to 150). Additionally,
170 Figure 1c indicates that abnormal fluctuations in Q5DOs induced by SPWs are not
171 equivalent to two oppositely propagating directions. An enhancement and a decrease in
172 the amplitudes of westward and eastward propagating Q5DOs can be simultaneously
173 observed. Results shown in Figure 1d are the same as that in Figure 1c but are derived
174 based on different phases of the westward and eastward Q5DOs in the synthetic data,
175 where $\pi/4$, and $-\pi/5$ are given in the westward and eastward Q5DOs. Comparing the
176 results between Figures 1c and 1d, it is interesting to note that the effect of a rapid large
177 change in SPWs on the derived Q5DOs also depends on the phase relationships.
178 Yamazaki and Matthias (2019) suggested that the effect of SPWs could be ignored when



179 the activities of Q10DWs in the oppositely propagating direction were not
180 simultaneously enhanced. However, according to our simulations, this criterion does
181 not suitable for the analysis of Q5DOs with different phases. Our simulation indicates
182 that the influence of a quick and large change of SPW should not be ignored when
183 extracting Q5DOs during SSWs from satellite observations based on the least square
184 fitting method. Thus, we develop a new fitting method to derive the Q5DOs by
185 suppressing the effect of a rapid and large change in SPWs.

186 **3.2 New fitting method**

187 Since the daily amplitude of SPW ($A_k(t)$) cannot be directly derived when
188 Q5DOs exist, the primary goal of the new method is to eliminate the rapid and large
189 changes in $A_k(t)$. The following steps are performed, where SPWs and Q5DOs are
190 considered within the same wavenumbers.

191 **Step 1. Estimate the daily variations of SPWs.**

192 Based on the definition of SPW, the phase φ_k should be a fixed value in each
193 window. Therefore, φ_k is first fitted based on $y(x) = a_k \cos(kx - \varphi_k)$, where $y(x)$
194 is the time-averaged geopotential height in each 20-day window. Using the fitted phase
195 φ_k , the daily amplitudes of SPW can be roughly estimated by the least square fitting
196 based on equation (2), which equals equation (1).

$$197 \quad Y(x, t) = [A_k(t) + B_w \cos(\omega t - \varphi_w + \varphi_k) + B_e \cos(\omega t - \varphi_e - \varphi_k)] \cos(kx - \varphi_k) \\ 198 \quad + [B_e \sin(\omega t - \varphi_e - \varphi_k) - B_w \sin(\omega t - \varphi_w + \varphi_k)] \sin(kx - \varphi_k) \quad (2)$$

199 If we let $a_k(t) = A_k(t) + B_w \cos(\omega t - \varphi_w + \varphi_k) + B_e \cos(\omega t - \varphi_e - \varphi_k)$, and
200 $b_k(t) = B_e \sin(\omega t - \varphi_e - \varphi_k) - B_w \sin(\omega t - \varphi_w + \varphi_k)$, equation (2) can be simply



201 expressed as equation (3):

$$202 \quad Y(x, t) = a_k(t) \cos(kx - \varphi_k) + b_k(t) \sin(kx - \varphi_k) \quad (3)$$

203 However, the fitted amplitudes of SPWs, $a_k(t)$, are not the true amplitudes of SPWs
204 ($A_k(t)$), which includes the aliasing from Q5DOs. According to the above two
205 equations, rapid and large changes in SPW amplitudes can only have impacts on the
206 values of $a_k(t)$. Because the true values of $A_k(t)$ cannot be directly fitted due to the
207 aliasing of Q5DOs, our goal in Step 2 is to eliminate the rapid large changes in $a_k(t)$.

208 **Step 2. Eliminate the large rapid changes in SPWs.**

209 If we let $P_k(t) = B_w \cos(\omega t - \varphi_w + \varphi_k) + B_e \cos(\omega t - \varphi_e - \varphi_k) =$
210 $P \cos(\omega t - \varphi)$, $a_k(t)$ in Equation (3) can be also expressed as,

$$211 \quad a_k(t) = A_k(t) + P_k(t) = A_k(t) + P \cos(\omega t - \varphi) \quad (4)$$

212 The amplitude P and phase φ can be estimated by the least square fitting via
213 equation (4). Taking the partial derivatives in time on both sides of equation (4), we
214 obtain equation (5):

$$215 \quad \frac{\partial}{\partial t} a_k(t) = \frac{\partial}{\partial t} A_k(t) + \frac{\partial}{\partial t} P_k(t) \quad (5)$$

216 where $\frac{\partial}{\partial t} A_k(t)$ are the daily variations in the amplitudes of SPW. The primary goal of
217 Step 2 is to subtract large values of $\frac{\partial}{\partial t} A_k(t)$ from $a_k(t)$ to eliminate the large
218 variations in $a_k(t)$. However, $\frac{\partial}{\partial t} A_k(t)$ cannot be obtained simply by $\frac{\partial}{\partial t} A_k(t) =$
219 $\frac{\partial}{\partial t} a_k(t) - \frac{\partial}{\partial t} P_k(t)$, because $\frac{\partial}{\partial t} P_k(t)$ cannot be derived accurately when $\left| \frac{\partial}{\partial t} A_k(t) \right|$
220 are large (“ $| \quad |$ ” represents the absolute values). Nevertheless, the lower boundary of
221 the values in $\left| \frac{\partial}{\partial t} a_k(t) \right|$ can be estimated when rapid large changes exist in SPWs
222 ($\left| \frac{\partial}{\partial t} A_k(t) \right|$ are large). The maximum value in $\left| \frac{\partial}{\partial t} a_k(t) \right|$ will be at least larger than the



223 maximum value in $\frac{\partial}{\partial t} P_k(t) = -\omega P \sin(\omega t - \varphi)$, which is ωP . Thus, the value of ωP
224 can be used as a threshold to determine rapid large changes in SPWs.

225 Therefore, when $\left| \frac{\partial}{\partial t} a_k(t) \right|$ are larger than the threshold of ωP , we subtract the
226 value of the corresponding $\frac{\partial}{\partial t} A_k(t)$ from all the following members of $a_k(t)$ to
227 obtain a new series of $a_k^{new}(t)$. The $\frac{\partial}{\partial t} A_k(t)$ are estimated by $\frac{\partial}{\partial t} A_k^{estimated}(t) =$
228 $\frac{\partial}{\partial t} a_k(t) - \frac{\partial}{\partial t} P_k^{estimated}(t)$, where $P_k^{estimated}(t) = P_{pre} \cos(\omega(t+1) - \varphi_{pre})$.
229 Instead of the P and φ fitted in the present window, the P_{pre} and φ_{pre} fitted from
230 the previous one are used because the fitted P_{pre} and φ_{pre} are not influenced by the
231 effect of rapid large changes in SPWs in the present window. Here, we have a new
232 series of $a_k^{new}(t)$ without rapid large changes in SPWs, as well as new fitted P and
233 φ for the next window.

234 **Step 3. Fit the real amplitudes of Q5DOs.**

235 After obtained the $a_k^{new}(t)$ and $b_k(t)$ from Step 2, the original data $Y'(x, t)$,
236 which inhibits the rapid and large changes in SPWs, can be reconstructed based on
237 equation (6):

$$238 \quad Y'(x, t) = a_k^{new}(t) \cos(kx - \varphi_k) + b_k(t) \sin(kx - \varphi_k) \quad (6)$$

239 Then, the real amplitudes and phases of the Q5DOs (B_w , B_e , φ_w , and φ_e) can be fitted
240 using the least square fitting method via $Y'(x, t) = B_w \cos(\omega t + kx -$
241 $\varphi_w) + B_e \cos(\omega t - kx - \varphi_e) + C$, where C is a constant.

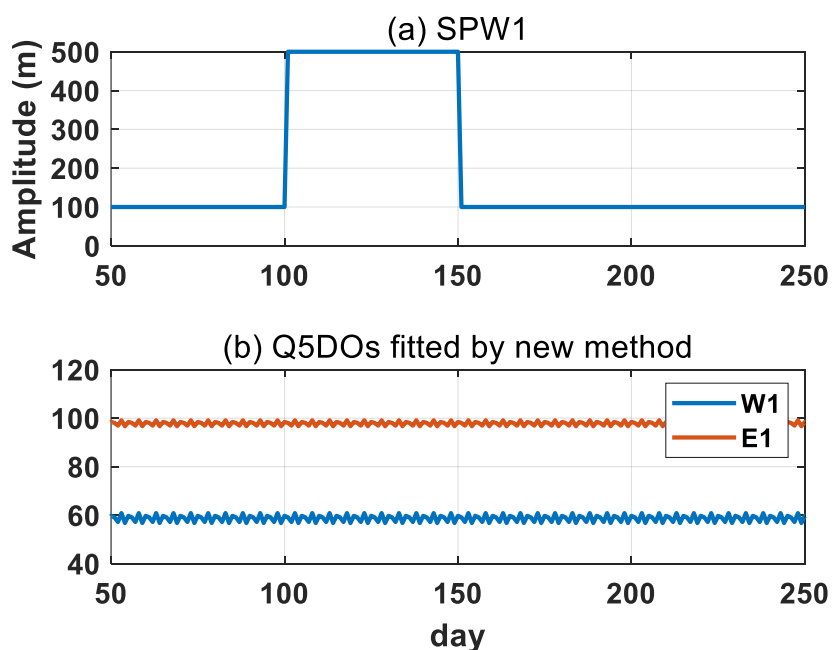
242 Note that, the effect of small changes in SPWs cannot be eliminated sometimes
243 when $\left| \frac{\partial}{\partial t} a_k(t) \right|$ are smaller than ωP . These small changes in SPWs do not have
244 significant effects on the fitted Q5DOs and their elimination depends on the phase



245 relationships between westward and eastward Q5DOs. Nevertheless, the Monte Carlo
246 simulation based on random phases of Q5DOs reveals that the fake fluctuations in
247 Q5DO amplitudes due to this effect will not exceed the value of $0.1\omega P$.

248 4. Results and Discussions

249 4.1 Simulations



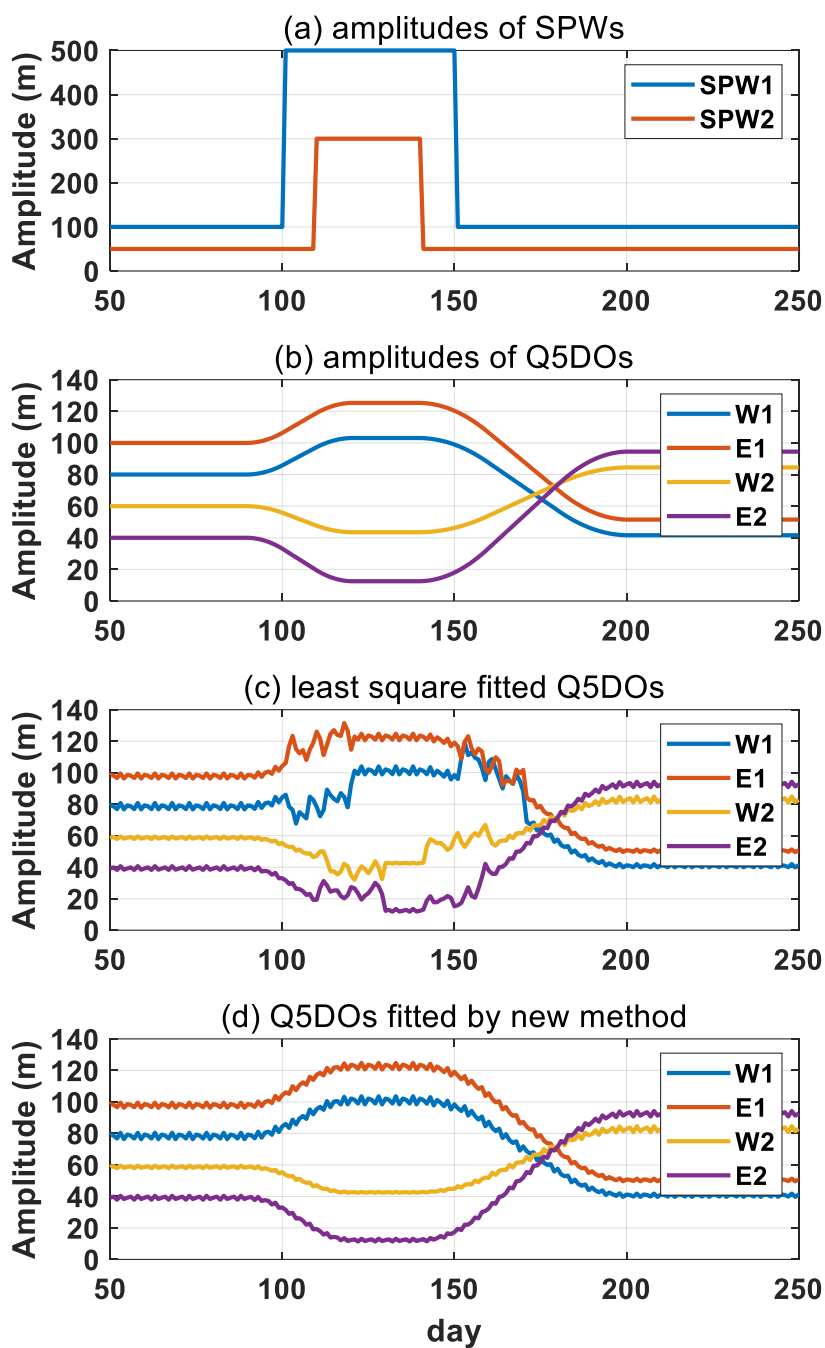
250

251 Figure 2. Simulations of the new fitting method based on synthetic data, which includes
252 an SPW and westward and eastward Q5DOs with zonal wavenumber of 1. (a) Daily
253 variations of the SPW amplitudes. The phase of the SPW is 0. (b) Q5DOs obtained from
254 the new fitting method. The amplitudes are 60 m and 100 m, the phases are $-\pi/4$ and
255 $\pi/5$ for the westward and eastward Q5DOs, respectively.

256 Based on the new fitting method, we present the fitting result in Figure 2. As shown



257 in Figure 2b, the fitted amplitudes of the Q5DOs are generally consistent with the
258 amplitudes given in the original synthetic data. The apparent fluctuations in Q5DOs
259 induced by SPWs have been removed. Note that, the fitting amplitudes of the new
260 method are the same as those shown in Figure 2b when Q5DOs have different phases
261 (not shown). Thus, the fitted amplitudes from the new method do not rely on the phase
262 relationships of those waves. Figure 2 demonstrates that the new method is effective to
263 suppress the effect of large rapid change in SPWs, while additional experiment where
264 synthetic data contain the enhancement of both SPWs and Q5DOs is needed to
265 demonstrate that the new method can properly capture the changes of Q5DOs during
266 SSWs. Besides, we also add signals of SPWs and Q5DOs with wavenumber 2 in the
267 synthetic data to establish a simulation that can model the real situation in satellite
268 observations. Figure 3 shows the results of an additional experiment. The synthetic data
269 used in Figure 3 consist of six components: SPWs with wavenumber 1 and 2 (SPW1
270 and SPW2), westward propagating Q5DOs with wavenumber 1 and 2 (W1 and W2),
271 and eastward propagating Q5DOs with wavenumber 1 and 2 (E1 and E2). The daily
272 variation of the amplitudes for SPWs and Q5DOs are separately shown in Figures 3a
273 and 3b. The phase of SPW1, SPW2, and W1, E1, W2, and E2 Q5DOs are respectively
274 set as 0 , $\pi/6$, $-\pi/4$, $\pi/5$, $-\pi/4$, and $\pi/3$. Figures 3c and 3d present the fitting results for the
275 least square fitting method and the new fitting method. As shown in Figure 3d, the result
276 manifests that the variations of Q5DOs can be captured based on the new method and
277 the effect of large rapid change in SPWs can be limited.





279 Figure 3. Simulations of the new fitting method based on synthetic data, which include
280 (a) SPW1 and SPW2 and (b) westward and eastward Q5DOs with zonal wavenumber
281 of 1 and 2. The phase of SPW1, SPW2, and W1, E1, W2, and E2 Q5DOs are
282 respectively set as 0 , $\pi/6$, $-\pi/4$, $\pi/5$, $-\pi/4$, and $\pi/3$. (c) Daily amplitudes of the fitted
283 Q5DOs obtained from the original least square fitting method. (d) Daily amplitudes of
284 the fitted Q5DOs obtained from the new fitting method.

285 4.2 Observations

286 Using the geopotential height data provided by the Aura/MLS measurement, we
287 extract the variations of the traveling Q5DOs at 60°N during Arctic SSWs. The
288 effectiveness of the new fitting method is discussed by comparing the results between
289 the original least square fitting method and the new method. The daily amplitudes of
290 the Q5DOs are obtained with the largest value in the wave periods between 4 and 7
291 days. The fitting result is marked at the end day of each 20-day window. The traveling
292 Q5DOs with wavenumber 3 and the amplitudes below 10 hPa are not shown due to
293 their weak amplitudes. In the present study, the pressure regions from 10 hPa to 1 hPa,
294 from 1 hPa to 0.01 hPa, and from 0.01 hPa to 0.001 hPa are respectively discussed as
295 the stratosphere, mesosphere, and lower thermosphere.

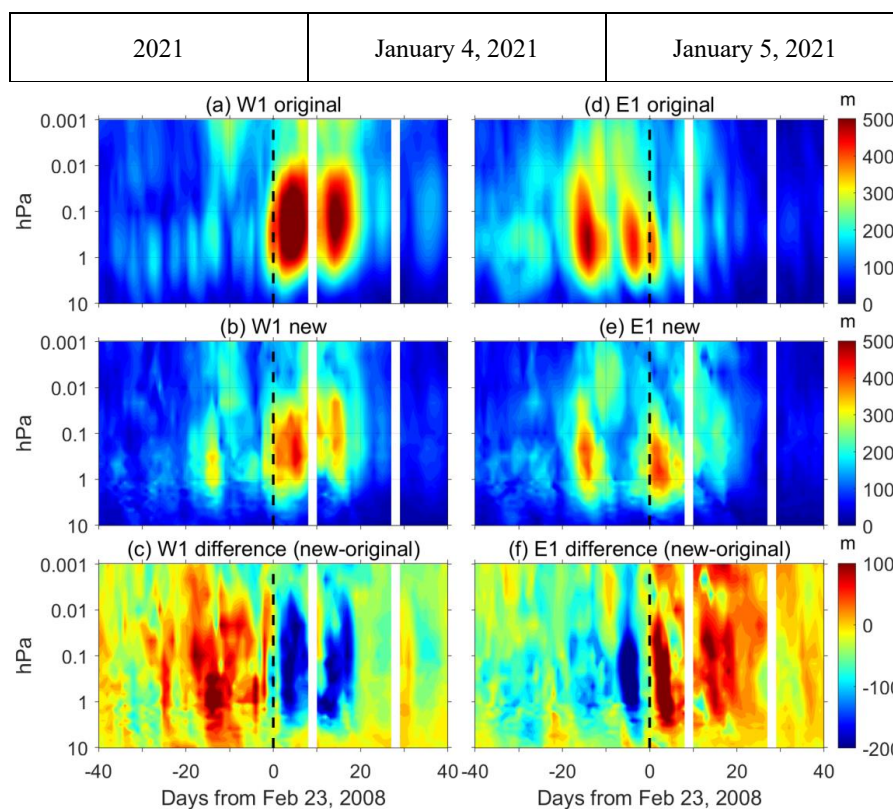
296 Since the observation of the Aura satellite is available after August 2004, the
297 variations of traveling Q5DOs are investigated during eight mid-winter major SSWs
298 from 2005 to 2021 in the present study. Table 1 presents the eight mid-winter major
299 SSWs with their onset dates. The date with the maximum positive temperature gradient
300 between 90°N and 60°N at 10 hPa is defined as the SSW onset date, which is obtained



301 around the date of the first wind reversal during each major event (e.g., Andrews et al.,
302 1987). Note that the onset date used in the present study is only to roughly determine
303 the commencement of SSWs and our discussions are not sensitive to the non-uniformed
304 definitions of SSW onsets (e.g., Butler et al., 2015). In the present study, the SSW in
305 the winter of 2009/2010 is classified as a minor one, because the wind reversal occurred
306 too late (18 days after the onset date) without any positive temperature gradient between
307 90°N and 60°N at 10 hPa. To be distinguished from the SSW in February 2018, the
308 SSW with the onset date of December 28, 2018, is discussed as the “2019 SSW” in this
309 study. The SSWs before 2013 have been widely studied in previous studies (e.g., Choi
310 et al., 2019; Charlton and Polvani, 2007; Butler et al., 2017), and details of the three
311 major SSWs from 2018 to 2021 can be referred to many recent reports (e.g., Rao et al.,
312 2018, 2020, 2021; Wang et al., 2019; Davis et al., 2022; Okui et al., 2021; Wright et al.,
313 2021).

314 Table 1. Mid-winter major SSWs from 2005 to 2021.

SSW	Onset Date	First Wind Reversal Date
2006	January 22, 2006	January 21, 2006
2007	February 24, 2007	February 24, 2007
2008	February 23, 2008	February 22, 2008
2009	January 23, 2009	January 24, 2009
2013	January 6, 2013	January 6, 2013
2018	February 11, 2018	February 12, 2018
2019	December 28, 2018	January 2, 2019



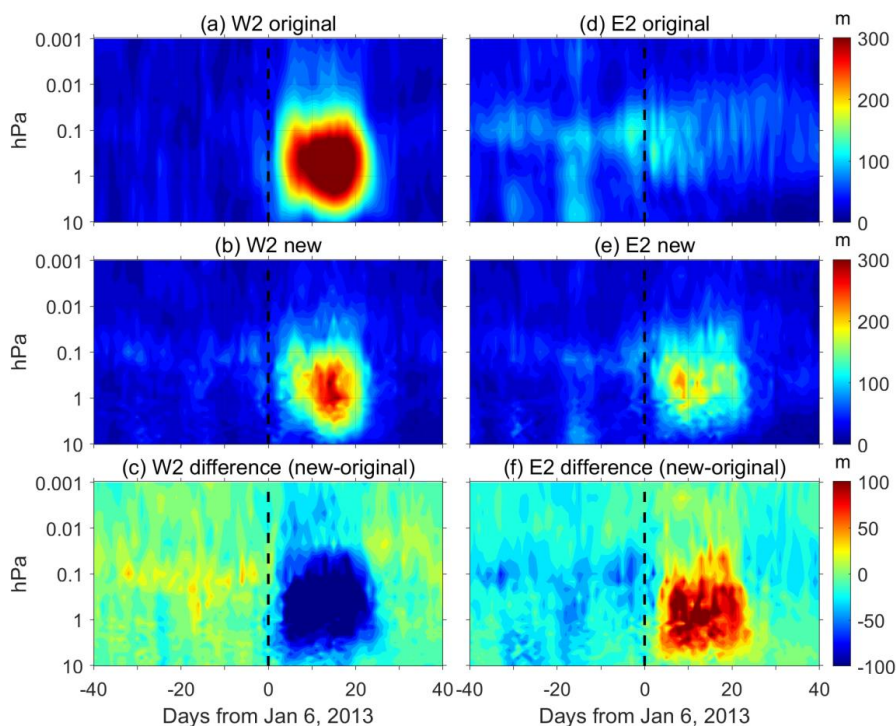
315

316 Figure 4. The amplitudes of W1 (left column) and E1 (right column) Q5DOs during the
 317 2008 SSW obtained by the original least square fitting method (top row) and the new
 318 fitting method (middle row). The differences between the new and original methods are
 319 shown in the bottom row (c and f). Contour steps are 10 m.

320 Comparisons of fitted amplitudes of traveling Q5DOs are firstly shown in Figures
 321 4 and 5, respectively for wavenumber 1 during the 2008 SSW and wavenumber 2 during
 322 the 2013 SSW. Results for each case are given in 81 days, which is from 40 days before
 323 to 40 days after the SSW onset date (day 0). Figure 4 presents the amplitudes of W1
 324 and E1 Q5DOs obtained from both original (top) and new (middle) methods during the
 325 2008 SSW. The differences are calculated by subtracting the fitting result of the original



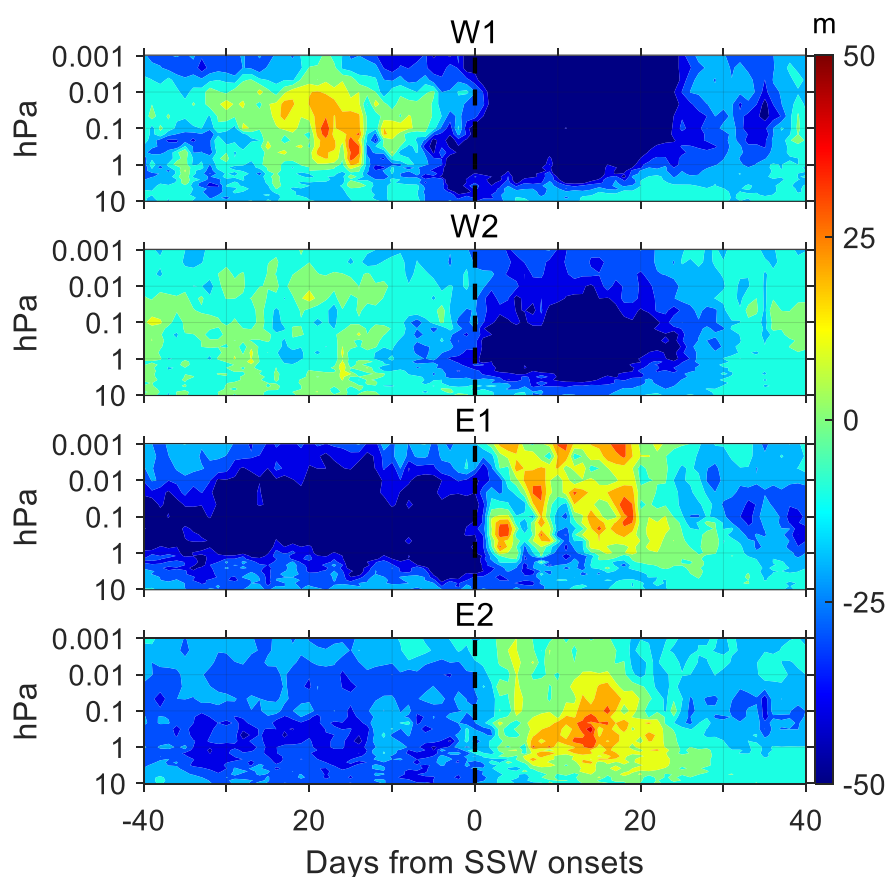
326 method from the new method, which are given at the bottom of Figure 4. Amplitudes
327 are not fitted in the white area where the available data are less than 60% in each
328 window. As shown in Figure 4a, the W1 Q5DOs fitted by the original least square fitting
329 method reveal a significant response to the onset of 2008 SSW. The amplitudes of the
330 W1 Q5DOs in the mesosphere are larger than 500 m from day 0 to day 20 with a
331 maximum amplitude of 628 m on day 5. Figure 4b suggests that the amplitudes obtained
332 from the new method are lower than 500 m during the 2008 SSW. The maximum
333 amplitude obtained from the new method is 466 m on day 5, which is about 75% of the
334 amplitude obtained from the original least square fitting method. The negative
335 differences shown in Figure 4c are generally larger than 200 m from day 0 to day 20 in
336 the mesosphere, which indicates that the amplitudes of W1 Q5DOs after the onset of
337 2008 SSW are largely overestimated by the original least square fitting method.
338 Nevertheless, positive differences larger than 100 m are also captured before the SSW
339 onset (day -15) around 1 hPa as shown in Figure 4c, which reveals that the amplitudes
340 of W1 Q5DOs obtained from the original method can be also underestimated during
341 the 2008 SSW. For the amplitudes of E1 Q5DOs during the 2008 SSW, the original
342 least square fitting method has an overestimation before the onset date and an
343 underestimation after the onset date. As shown in Figure 4f, the positive and negative
344 differences both have maximum amplitudes over 200 m in the mesosphere around the
345 onset date.



346

347 Figure 5. Same as Figure 4 but for W2 and E2 Q5DOs during the 2013 SSW.

348 Figure 5 presents the same results as Figure 4 but for the amplitudes of W2 and
349 E2 Q5DOs during the 2013 SSW. As shown in Figure 5, strong enhancements of W2
350 Q5DOs and weak amplitudes of E2 Q5DOs after the 2013 SSW are captured by the
351 original least square fitting method. However, results from the new method after the
352 onset of 2013 SSW suggest that the amplitudes of W2 Q5DOs are overestimated and
353 the E2 Q5DOs are underestimated. The maximum positive and negative differences are
354 both over 100 m. In order to understand the common differences between the two
355 methods, we calculate the differences during all the eight SSWs and present a composite
356 result in Figure 6.



357
358 Figure 6. The differences between the new and original methods for the W1, W2, E1,
359 and E2 Q5DOs (from top to bottom). Contour steps are 10 m.

360 As shown in Figure 6, the westward propagating Q5DOs are usually overestimated
361 by the original least square fitting method after the SSW onsets, while the eastward
362 propagating Q5DOs are mostly underestimated after the SSW onsets. The E1 Q5DOs
363 before the SSW onsets are also overestimated by the original least square fitting method
364 as seen in Figure 6c. The enhancements of traveling Q5DOs during SSWs reported in
365 previous studies are usually westward propagating after the SSW onsets and eastward



366 propagating before the SSW onsets (e.g., Gong et al., 2018; Yu et al., 2022). Thus, our
367 analyses indicate that the previously-reported Q5DOs obtained by satellite
368 measurements during SSWs might be contaminated by SPWs. The amplitudes of the
369 enhancement of Q5DOs during SSWs might be overestimated. Additionally, Figure 6
370 reveals that the westward propagating Q5DOs before the SSW onsets and the eastward
371 propagating Q5DOs after the SSW onsets are underestimated by the original least
372 square fitting method. Therefore, in future studies of the activities of Q5DOs during
373 SSWs based on satellite observations and reanalysis data, the variations of different
374 wave components in Q5DOs have to be carefully derived by eliminating the effects of
375 SPWs.

376 **5. Summary and conclusions**

377 In the present study, a new fitting method is developed to derive the variations of
378 traveling quasi-5-day waves (Q5DOs) by inhibiting the effect of rapid and large
379 changes in the amplitudes of stationary planetary waves (SPWs). The effectiveness of
380 the new method is demonstrated by both synthetic and observational data. According
381 to the simulations, the new method can capture the variations of the amplitudes of
382 traveling Q5DOs when large and rapid changes in SPWs are given. Based on the
383 geopotential height data measured by MLS onboard the Aura satellite, we compare the
384 difference of the traveling Q5DOs amplitudes between the original least square fitting
385 method and the new fitting method in the middle atmosphere during eight Arctic major
386 SSWs from 2005 to 2021. Our results indicate that the enhancements of traveling



387 Q5DOs during SSWs reported in previous studies might be overestimated due to
388 ignoring the effect of large rapid changes in SPWs. Besides, the amplitudes of westward
389 propagating Q5DOs before the SSW onsets and the amplitudes of eastward propagating
390 Q5DOs after the SSW onsets might be underestimated. Note that since the amplitudes
391 of SPWs cannot be derived accurately due to the aliasing of Q5DOs, the contribution
392 of the SPWs and Q5DOs during SSWs cannot be quantified in the present method. Our
393 goal is to attenuate the effect of SPWs on the derivation of Q5DOs during SSWs.
394 Future works are needed to examine the effectiveness of the new method by using
395 traveling planetary oscillations with other periods, such as the quasi-10-day and quasi-
396 16-day waves.

397

398 **Data availability.** The Aura/MLS geopotential height data can be downloaded through
399 the Goddard Earth Sciences Data and Information Services Center via
400 (https://acdsc.gesdisc.eosdis.nasa.gov/data/Aura_MLS_Level2/ML2GPH.004/).

401

402 **Author contributions.** ZM and YG proposed the scientific ideas. QX and ZM
403 contributed to data processing and simulation programming. ZM, YG, and SZ
404 completed the analysis and manuscript. CH and KH discussed the results in the
405 manuscript.

406

407 **Competing interests.** The authors declare that they have no conflict of interest.

408



409

410 **Acknowledgments.** We acknowledge the Goddard Earth Sciences Data and
411 Information Services Center for providing the Aura/MLS geopotential height data.

412

413 **Financial support.** This study is supported by the National Natural Science Foundation
414 of China (through grants 42104145 and 41574142), the Fundamental Research Funds
415 for the Central Universities 2042021kf0021, and the China Postdoctoral Science
416 Foundation (through grants 2021M692465 and 2020TQ0230).

417

418

419 **References**

420 Andrews, D. G., Holton, J. R., and Leovy, C. B.: Middle Atmosphere Dynamics, 1st
421 ed., Academic Press, San Diego, Calif, 1987.

422 Baldwin, M. P., Ayarzagüena, B., Birner, T., Butchart, N., Butler, A. H., and Charlton-
423 Perez, A. J.: Sudden stratospheric warmings. Reviews of Geophysics, 58,
424 e2020RG000708. <https://doi.org/10.1029/2020RG000708>, 2020.

425 Butler, A. H., Seidel, D. J., Hardiman, S. C., Butchart, N., Birner, T., and Match, A.:
426 Defining Sudden Stratospheric Warmings, Bulletin of the American
427 Meteorological Society, 96(11), 1913-1928, [https://doi.org/10.1175/BAMS-D-13-
428 00173.1](https://doi.org/10.1175/BAMS-D-13-00173.1), 2015.

429 Butler, A. H., Sjoberg, J. P., Seidel, D. J., and Rosenlof, K. H.: A sudden stratospheric



- 430 warming compendium. *Earth System Science Data*, 9, 63–76.
431 <https://doi.org/10.5194/essd-9-63-2017>, 2017.
- 432 Charlton, A. J., and Polvani, L. M.: A new look at stratospheric sudden warmings. Part
433 I: Climatology and modeling benchmarks. *J. Climate*, 20(3), 449–469.
434 <https://doi.org/10.1175/JCLI3996.1>, 2007.
- 435 Choi, H., Kim, B. M., and Choi, W.: Type classification of sudden stratospheric
436 warming based on pre- and postwarming periods. *Journal of Climate*, 32(8), 2349–
437 2367. <https://doi.org/10.1175/JCLI-D-18-0223.1>, 2019
- 438 Davis, N.A., Richter, J.H., Glanville, A.A., Edwards, J., and LaJoie, E.: Limited surface
439 impacts of the January 2021 sudden stratospheric warming. *Nature*
440 *Communications*, 13, 1136. <https://doi.org/10.1038/s41467-022-28836-1>, 2022.
- 441 Domeisen, D. I. V., Butler, A. H., Charlton-Perez, A. J., Ayarzagüena, B., Baldwin, M.
442 P., Dunn-Sigouin, E., Furtado, J. C., Garfinkel, C. I., Hitchcock, P., Karpechko, A.
443 Yu., Kim, H., Knight, J., Lang, A. L., Lim, E., Marshall, A., Roff, G., Schwartz,
444 C., Simpson, I. R., Son, S., Taguchi, M.: The role of the stratosphere in subseasonal
445 to seasonal prediction: 2. Predictability arising from stratosphere-troposphere
446 coupling. *Journal of Geophysical Research: Atmospheres*, 125, e2019JD030923.
447 <https://doi.org/10.1029/2019JD030923>, 2020.
- 448 Gong, Y., Li, C., Ma, Z., Zhang, S., Zhou, Q., Huang, C., Huang, K., Li, G., Ning, B.:
449 Study of the quasi-5-day wave in the MLT region by a meteor radar chain. *Journal*
450 *of Geophysical Research: Atmospheres*, 123, 9474–9487.



- 451 <https://doi.org/10.1029/2018JD029355>, 2018.
- 452 Gong, Y., Wang, H., Ma, Z., Zhang, S., Zhou, Q., Huang, C., and Huang, K.: A statistical
453 analysis of the propagating quasi 16-day waves at high latitudes and their response
454 to sudden stratospheric warmings from 2005 to 2018. *Journal of Geophysical*
455 *Research: Atmospheres*, 124, 12,617–12,630.
456 <https://doi.org/10.1029/2019JD031482>, 2019.
- 457 Huang, Y. Y., Zhang, S., Li, C. Y., Li, H. J., Huang, K., and Huang, C.: Annual and inter-
458 annual variations in global 6.5DWs from 20–110 km during 2002–2016 observed
459 by TIMED/SABER. *Journal of Geophysical Research: Space Physics*, 122, 8985–
460 9002. <https://doi.org/10.1002/2017JA023886>, 2017.
- 461 King, A. D., Butler, A. H., Jucker, M., Earl, N. O., and Rudeva, I.: Observed
462 relationships between sudden stratospheric warmings and European climate
463 extremes. *Journal of Geophysical Research: Atmospheres*, 124(24), 13943–13961.
464 <https://doi.org/10.1029/2019JD030480>, 2019.
- 465 Koushik, N., Kumar, K. K., Ramkumar, G., Subrehmanyam, K. V., Kishore Kumar, G.,
466 Hocking, W. K., He, M., Latteck, R.: Planetary waves in the mesosphere lower
467 thermosphere during stratospheric sudden warming: Observations using a network
468 of meteor radars from high to equatorial latitudes. *Climate Dynamics*, 54(9–10),
469 4059–4074. <https://doi.org/10.1007/s00382-020-05214-5>, 2020.
- 470 Kozubek, M., Krizan, P., and Lastovicka, J.: Northern Hemisphere stratospheric winds
471 in higher midlatitudes: longitudinal distribution and long-term trends. *Atmos.*



- 472 Chem. Phys., 15(4), 2203–2213. <https://doi.org/10.5194/acp-15-2203-2015>, 2015.
- 473 Lawrence, Z. D., and Manney, G. L.: Characterizing stratospheric polar vortex
474 variability with computer vision techniques. *Journal of Geophysical Research:*
475 *Atmospheres*, 123(3), 1510–1535., 2018.
- 476 Lin, J. T., Lin, C. H., Rajesh, P. K., Yue, J., Lin, C. Y., and Matsuo, T.: Local-time and
477 vertical characteristics of quasi-6-day oscillation in the ionosphere during the 2019
478 Antarctic sudden stratospheric warming. *Geophysical Research Letters*, 47.
479 <https://doi.org/10.1029/2020GL090345>, 2020.
- 480 Livesey, N. J., Read, W. G., Wagner, P. A., Froidevaux, L., Lambert, A., Manney, G. L.,
481 Millan Valle, L. F., Pumphrey, H. C., Santee, M. L., Schwartz, M. J., Wang, S.,
482 Fuller, R. A., Jarnot, R. F., Knosp, B. W., and Martinez, E.: Earth Observing
483 System (EOS) Aura Microwave Limb Sounder (MLS) Version 4.2x Level 2 data
484 quality and description document, Tech. Rep. D-33509 Rev. A, JPL, 2015.
- 485 Liu, H. L., Talaat, E. R., Roble, R. G., Lieberman, R. S., Riggin, D. M., and Yee, J. H.:
486 The 6.5-day wave and its seasonal variability in the middle and upper atmosphere.
487 *Journal of Geophysical Research*, 109, D21112.
488 <https://doi.org/10.1029/2004JD004795>, 2004.
- 489 Longuet-Higgins, M. S.: The eigenfunctions of Laplace’s tidal equations over a sphere,
490 *Philosophical Transactions of the Royal Society of London*. 262, 511-607.
491 doi:10.1098/rsta.1968.0003, 1968.
- 492 Ma, Z., Gong, Y., Zhang, S., Zhou, Q., Huang, C., Huang, K., Luo, J., Yu, Y., Li, G.:



- 493 Study of a quasi-4-day oscillation during the 2018/2019 SSW over Mohe, China.
494 Journal of Geophysical Research: Space Physics, 125, e2019JA027687.
495 <https://doi.org/10.1029/2019JA027687>, 2020.
- 496 Ma, Z., Gong, Y., Zhang, S., Xiao, Q., Xue, J., Huang, C., and Huang, K.:
497 Understanding the excitation of quasi-6-day waves in both hemispheres during the
498 September 2019 Antarctic SSW. Journal of Geophysical Research: Atmospheres,
499 127, e2021JD035984. <https://doi.org/10.1029/2021JD035984>, 2022.
- 500 Manney, G. L., Schwartz, M. J., Krüger, K., Santee, M. L., Pawson, S., Lee, J. N., Daffer,
501 W. H., Fuller, R. A., and Livesey, N. J.: Aura Microwave Limb Sounder
502 observations of dynamics and transport during the record breaking 2009 Arctic
503 stratospheric major warming. Geophys. Res. Lett., 36(12), L12815.
504 <https://doi.org/10.1029/2009GL038586>, 2009.
- 505 Matsuno, T.: A dynamical model of the stratospheric sudden warming. Journal of the
506 Atmospheric Sciences, 28, 1479–1494. [https://doi.org/10.1175/1520-0469\(1971\)028<1479:ADMOTS>2.0.CO;2](https://doi.org/10.1175/1520-0469(1971)028<1479:ADMOTS>2.0.CO;2), 1971.
- 508 Okui, H., Sato, K., Koshin, D., and Watanabe, S.: Formation of a mesospheric inversion
509 layer and the subsequent elevated stratopause associated with the major
510 stratospheric sudden warming in 2018/19. Journal of Geophysical Research:
511 Atmospheres, 126, e2021JD034681. <https://doi.org/10.1029/2021JD034681>,
512 2021.
- 513 Pancheva, D., Mukhtarov, P., and Siskind, D. E.: The quasi-6-day waves in NOGAPS-



- 514 ALPHA forecast model and their climatology in MLS/Aura measurements (2005-
515 2014), *Journal of Atmospheric and Solar-Terrestrial Physics*, 181, 19-37,
516 <https://doi.org/10.1016/j.jastp.2018.10.008>, 2018.
- 517 Qin, Y., Gu, S-Y., Teng, C-K-M., Dou, X-K., Yu, Y., and Li, N.: Comprehensive study
518 of the climatology of the quasi-6-day wave in the MLT region based on aura/MLS
519 observations and SDWACCM-X simulations. *Journal of Geophysical Research:*
520 *Space Physics*, 126, e2020JA028454. <https://doi.org/10.1029/2020JA028454>,
521 2021.
- 522 Rao, J., Garfinkel, C. I., and White, I. P.: Predicting the downward and surface influence
523 of the February 2018 and January 2019 sudden stratospheric warming events in
524 subseasonal to seasonal (S2S) models. *Journal of Geophysical Research:*
525 *Atmospheres*, 125, e2019JD031919. <https://doi.org/10.1029/2019JD031919>,
526 2020.
- 527 Rao, J., Ren, R., Chen, H., Yu, Y., and Zhou, Y.: The stratospheric sudden warming
528 event in February 2018 and its prediction by a climate system model. *Journal of*
529 *Geophysical Research: Atmospheres*, 123, 13,332–13,345.
530 <https://doi.org/10.1029/2018JD028908>, 2018.
- 531 Rao, J., Garfinkel, C. I., Wu, T., Lu, Y., Lu, Q., and Liang, Z.: The January 2021 sudden
532 stratospheric warming and its prediction in subseasonal to seasonal models.
533 *Journal of Geophysical Research: Atmospheres*, 126, e2021JD035057.
534 <https://doi.org/10.1029/2021JD035057>, 2021.



- 535 Rhodes, C. T., Limpasuvan, V., and Orsolini, Y. J.: Eastward-propagating planetary
536 waves prior to the January 2009 sudden stratospheric warming. *Journal of*
537 *Geophysical Research: Atmospheres*, 126, e2020JD033696.
538 <https://doi.org/10.1029/2020JD033696>, 2021.
- 539 Seviour, W. J. M., Mitchell, D. M., and Gray, L. J.: A practical method to identify
540 displaced and split stratospheric polar vortex events. *Geophys. Res. Lett.*, 40(19),
541 5268–5273. <https://doi.org/10.1002/grl.50927>, 2013.
- 542 Tunbridge, V. M., Sandford, D. J., and Mitchell, N. J.: Zonal wave numbers of the
543 summertime 2 day planetary wave observed in the mesosphere by EOS Aura
544 Microwave Limb Sounder. *J. Geophys. Res.*, 116, D11103,
545 doi:10.1029/2010JD014567, 2011.
- 546 Wang, J. C., Palo, S. E., Forbes, J. M., Marino, J., Moffat-Griffin, T., and Mitchell, N.
547 J.: Unusual quasi 10-day planetary wave activity and the ionospheric response
548 during the 2019 Southern Hemisphere sudden stratospheric warming. *Journal of*
549 *Geophysical Research: Space Physics*, 126, e2021JA029286.
550 <https://doi.org/10.1029/2021JA029286>, 2021.
- 551 Wang, Y., Shulga, V., Milinevsky, G., Patoka, A., Evtushevsky, O., Klekociuk, A., Han,
552 W., Grytsai, A., Shulga, D., Myshenko, V., and Antyufeyev, O.: Winter 2018 major
553 sudden stratospheric warming impact on midlatitude mesosphere from microwave
554 radiometer measurements. *Atmos. Chem. Phys.*, 19, 10303–10317,
555 <https://doi.org/10.5194/acp-19-10303-2019>, 2019.



- 556 Wright, C. J., Hall, R. J., Banyard, T. P., Hindley, N. P., Krisch, I., Mitchell, D. M., and
557 Seviour, W. J. M.: Dynamical and surface impacts of the January 2021 sudden
558 stratospheric warming in novel Aeolus wind observations, MLS and ERA5,
559 Weather Clim. Dynam., 2, 1283–1301, <https://doi.org/10.5194/wcd-2-1283-2021>,
560 2021.
- 561 Wu, D. L., Hays, P. B., and Skinner, W. R.: A least-squares method for spectral-analysis
562 of space-time series, J. Atmos. Sci., 52, 3501–3511, [https://doi.org/10.1175/1520-0469\(1995\)052<3501:ALSMFS>2.0.CO;2](https://doi.org/10.1175/1520-0469(1995)052<3501:ALSMFS>2.0.CO;2), 1995.
- 564 Yamazaki, Y., and Matthias, V.: Large-amplitude quasi-10-day waves in the middle
565 atmosphere during final warmings. Journal of Geophysical Research:
566 Atmospheres, 124, 9874–9892. <https://doi.org/10.1029/2019JD030634>, 2019.
- 567 Yamazaki, Y., Matthias, V., Miyoshi, Y., Stolle, C., Siddiqui, T., Kervalishvili, G.,
568 Laštovička, J., Kozubek, M., Ward, W., Themens, D. R., Kristoffersen, S., Alken,
569 P.: September 2019 Antarctic sudden stratospheric warming: Quasi-6-day wave
570 burst and ionospheric effects. Geophysical Research Letters, 47, e2019GL086577.
571 <https://doi.org/10.1029/2019GL086577>, 2020.
- 572 Yamazaki, Y., Matthias, V., and Miyoshi, Y.: Quasi-4-day wave: Atmospheric
573 manifestation of the first symmetric Rossby normal mode of zonal wavenumber 2.
574 Journal of Geophysical Research: Atmospheres, 126, e2021JD034855.
575 <https://doi.org/10.1029/2021JD034855>, 2021.
- 576 Yu, F. R., Huang, K. M., Zhang, S. D., Huang, C. M., and Gong, Y.: Observations of



577 eastward propagating quasi 6-day waves from the troposphere to the lower
578 thermosphere during SSWs in early 2016. Journal of Geophysical Research:
579 Atmospheres, 127, e2021JD036017, <https://doi.org/10.1029/2021JD036017>,
580 2022.
581